Birefringence properties of magneto-optic rib waveguide as a function of refractive index

Abdesselam Hocini · Ahmed Bouchelaghem · Djamel Saigaa · Mounir Bouras · Touraya Boumaza · Mohamed Bouchemat

Abstract We report on the theoretical study of magneto optical rib waveguides with two kinds of silica type matrix doped by magnetic nanoparticles and made by sol–gel process (SiO_2/ZrO_2 film or SiO_2/TiO_2). The mode propagation and the light confinement are simulated using software based on a Film Mode Matching method. The modeling is based on geometrical adjustments of the rib waveguide. We propose from those results magneto optical waveguide geometries for optical integrated applications.

Keywords Magneto optic · Birefringence · Rib waveguide · Integrated optics

1 Introduction

In an effort to find low-cost alternatives for components currently used in optical devices that have a nonreciprocal effect such as optical isolators and circulators.

The nonreciprocal behavior of these devices is based on the magneto-optic Faraday effect which occurs in magnetic garnet crystals [1–3]. The sol–gel process gives a solution to fabricate integrated optic devices. It is considered as a versatile, flexible and a low-cost technique useful for the realization of integrated photonic devices [4–8].

A. Hocini (✉) · A. Bouchelaghem · D. Saigaa · M. Bouras
Département d'Electronique, Faculté de Technologie, Université de M'sila, BP. 166, Route Ichebilia, M'sila 28000, Algeria
e-mail: hocini74@yahoo.fr

A. Hocini · T. Boumaza · M. Bouchemat
Laboratoire Micro-systèmes et Instrumentation (LMI), Université Mentouri, Constantine, Algeria

Currently, only bulk forms of these components made of garnet oxide crystals are commercially available, this class of material can not be easily integrated with standard fabrication technologies, and integrated versions are highly desirable. To overcome this problem, a large number of papers [5–8] are currently demonstrating the use of magnetic nanoparticles as magneto-optical active element in a silica-based matrix prepared via sol–gel process [7, 9]. This latter is prepared via organic-inorganic process. The attractivity of such approach lies in the full compatibility of the sol–gel coating with classical integrated technologies and especially the technology on glass. Furthermore, this elaboration method is easy to implement and provide magneto-optical thin films with a refractive index value (1,5) close to that of other integrated optical devices. The inherent low refractive index contrast between the film and the substrate in sol–gel organic inorganic waveguides combined with a thickness larger than that of classical magneto-optical waveguides, it should allow an efficient fiber coupling which is highly desirable for laser-waveguide coupling [5, 7].

The zero birefringence between the fundamental TE and TM modes is an essential condition in magneto optical rib wave guides. The Faraday rotation is observed in magneto optic waveguide and causes the mode conversion between TE and TM guided modes, but its efficiency is strongly affected by the difference between their propagation constant $\Delta\beta = \beta_{TE} - \beta_{TM}$ (the birefringence between TE and TM modes $\Delta Nm = (\beta_{TE} - \beta_{TM})\lambda/2\pi$). Indeed, the maximum TE–TM mode conversion ratio R_{max} induced by the Faraday effect is expressed as [7]:

$$R = \frac{\theta_F^2}{\theta_F^2 + (\Delta\beta/2)^2} \qquad (1)$$

θ_F (°/cm) is the specific Faraday rotation of the material constituting the waveguide.

Fig. 1 Schematic representation of a Rib waveguide. Structural parameters are the height h and the width w and refractive-index n_s, n_f, x and y denote the cross section coordinate axes, with the y-direction parallel to the substrate surface

Table 1 Refractive index of the host matrix at 1550 nm [9]

Ratio SiO$_2$/ZrO$_2$ or TiO$_2$	Precursors	Index @ 1550 nm
Sol 10/3	SiO$_2$, ZrO$_2$	1.504
Sol 10/7	SiO$_2$, ZrO$_2$	1.515
Sol 10/10	SiO$_2$, ZrO$_2$	1.528
Sol 10/12	SiO$_2$, TiO$_2$	1.580
Sol 10/10	SiO$_2$, TiO$_2$	1.575

The present work describes the design rule that must be imposed to the geometry and refractive index difference of such device to make them behave as TE/TM polarization free rib waveguides. It consists of the tuning the contrast and the etch depth of the rib which is a critical parameter in the design of rib waveguide [10, 11]. For a given wavelength, refractive index difference, the etch depth and the width of the waveguide are the only free parameter to adjust the realization of the birefringence free condition (phase matching condition). Since the dimension of a waveguide (height, width, and etching depth) is generally specified by technological requirements, the refractive index preferably should be adjustable. This is the subject of investigation of the present study.

2 Design structure

Design and simulation become very important before fabrication; the film mode matching (FMM) method by Sudbo [12, 13], which is full vectorial 3-D-mode solver has been used to study the influence of the geometrical parameters for the waveguide. The device is shown schematically in Fig. 1 where W is the rib width, H is the inner rib height, r is the fractional height of the side regions compared to the rib center (the outer–inner ratio). For a better understanding, we will also consider the etching depth $D = H(1 - r)$ which directly gives the edge height of the rib waveguide. We have chosen waveguide optical parameters corresponding to SiO$_2$/ZrO$_2$ film or SiO$_2$/TiO$_2$ doped with magnetic nanoparticles, the magneto-optical permittivity tensor ε_{mo} of the thin film is written in coordinate system $\{x, y, z\}$ by [14]:

$$\varepsilon_{mo} = \begin{bmatrix} \varepsilon_{xx} & +\varepsilon_{xy} & 0 \\ -\varepsilon_{xy} & \varepsilon_{xx} & 0 \\ 0 & 0 & \varepsilon_{xx} \end{bmatrix} \qquad (2)$$

where each element of tensor $\varepsilon_i = \varepsilon_i' + i\varepsilon_i''$ has real and imaginary parts where $i = xx$ or xy. The diagonal part, represents the permittivity tensor of isotropic medium:

$$\varepsilon_{xx}' = n^2 - k^2 \qquad (3)$$

and

$$\varepsilon_{xx}'' = 2nk \qquad (4)$$

where n is the refractive index of material and k is the extinction coefficient.

However, the application of a magnetic field on a material with a direction parallel to the light beam (Oz) produces an off-diagonal elements where the magnitude depends on the kind of material (on the Faraday rotation θ_F and ellipticity ε_F) [14].

$$\varepsilon_{xy}' = \frac{\lambda}{\pi}(n\theta_F - k\varepsilon_F) \qquad (5)$$

and

$$\varepsilon_{xy}'' = \frac{\lambda}{\pi}(n\theta_F + k\varepsilon_F) \qquad (6)$$

where λ is the wavelength, and by adjusting the molar ratio of metallic precursors the refractive index of the material can be varied in range of 1.51 to 1.58 [9].

This flexibility of the refractive index will be helpful to suit the optical characteristics of the magneto-optical film with requirements of the desired application. Table 1 shows that the refractive index of the host matrix.

3 Results and discussions

We fixed the rib-waveguide height parameter H to 3 µm, this dimension was chosen in order to maintain as large a device as possible for ease of coupling light to the device.

The effective indices for both fundamental quasi-TE and quasi-TM modes and their difference were calculated while keeping constant the refractive index of the host matrix n, the etch depth D (parameter r), and slab height h of the waveguide and changed the waveguide width to calculate the effective indices of the fundamental TE and TM waveguide modes.

The iteration of the simulation was repeated for a given values of the parameter r (etch depth). Hence, the process is one in which we determine the effective indices of the fundamental TE and TM waveguide modes as the waveguide width is gradually increased, and a series of ΔN points were calculated at wavelength 1.55 µm.

Fig. 2 Effective-index difference calculation between quasi-TE and quasi-TM polarized modes using FMM, for refractive index of the host matrix $n = 1.51$ at $\lambda = 1550$ nm
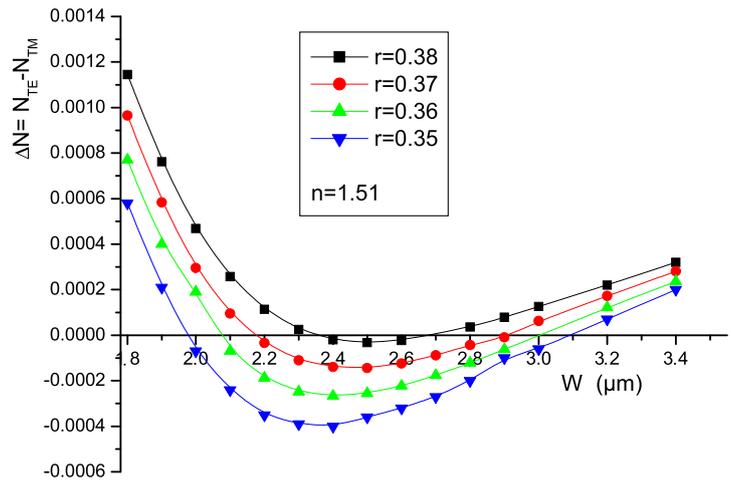
Fig. 3 Effective-index difference calculation between quasi-TE and quasi-TM polarized modes using FMM, for refractive index of the host matrix $n = 1.53$ at $\lambda = 1550$ nm
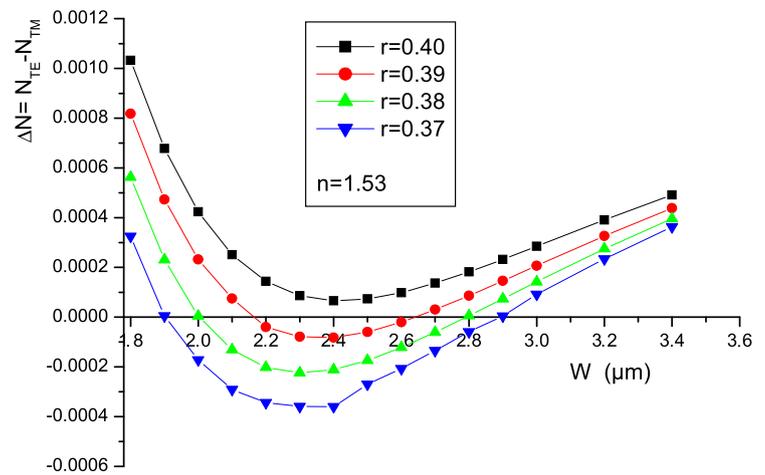
Fig. 4 Effective-index difference calculation between quasi-TE and quasi-TM polarized modes using FMM, for refractive index of the host matrix $n = 1.56$ at $\lambda = 1550$ nm
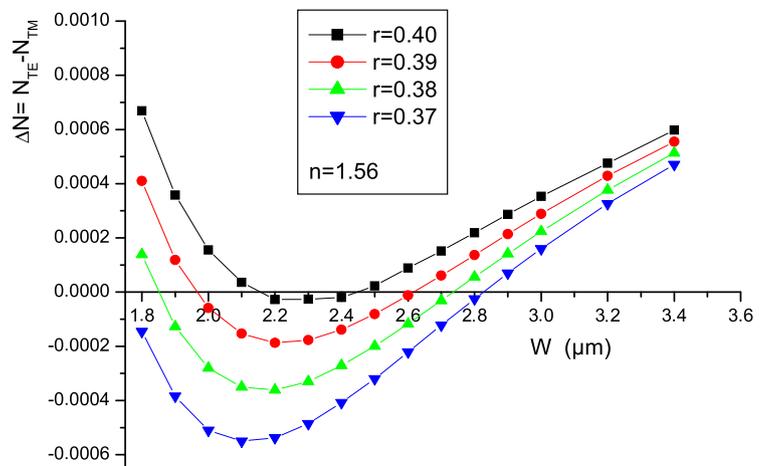
Figures 2, 3 and 4 show the plot of the birefringence as a function of the width W for different parameter r, for $n = 1.51, 1.53$ and 1.56. The results show that for greater values of parameter r (smaller values of etch depths D) the birefringence is always positive. The fundamental quasi-TE and quasi-TM waveguide modes cannot be equalized by varying values of waveguide width, and as the parameter r decreases (etch depth increases) a tendency for two specific values of waveguide widths for which the effective index of the fundamental quasi-TE and quasi-TM waveguide modes

Fig. 5 Effective-index difference calculation between quasi-TE and quasi-TM polarized modes using FMM, for $r = 0.38$ for different values of refractive index at $\lambda = 1550$ nm
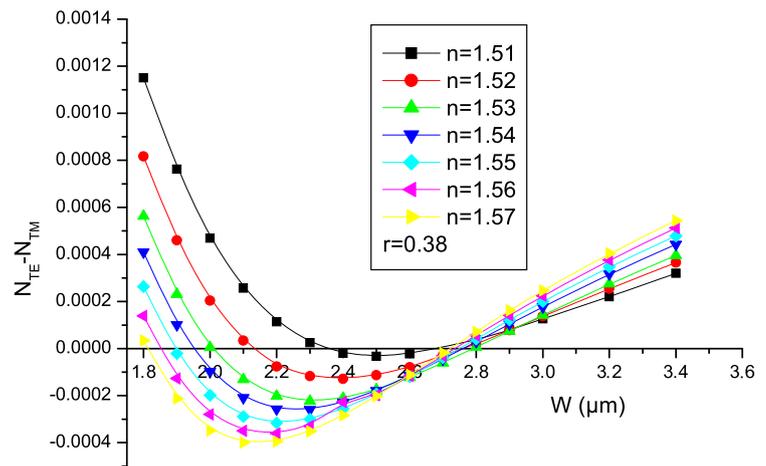
Fig. 6 Waveguide width influence on etching depth in the structure to support zero birefringence for refractive index of the host matrix $n = 1.51$, $n = 1.52$, $n = 1.53$, $n = 1.55$ and $n = 1.57$ at $\lambda = 1550$ nm
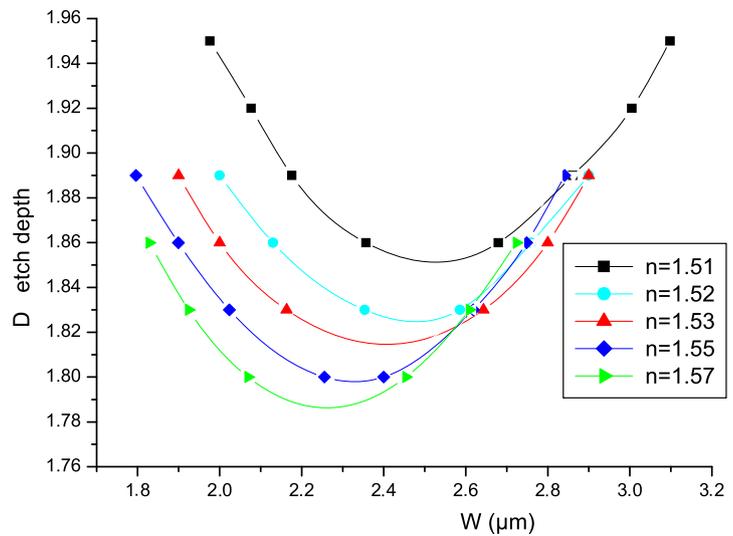
can be equalized. The intersection of the curves with the axe zero indicates that both TE and TM polarizations have the same effective index.

Assuming fabrication tolerances of 10 nm on the etching depth and for a Faraday rotation of 200 °/cm, this leads to a change in conversion ratio of about 2 %, which is quite acceptable.

For more details of the effect of refractive index on birefringence, we plot on Fig. 5, keeping the waveguide etch depth constant during the simulation, the influence of the waveguide width on the birefringence for various refractive index at the operating wavelength of $\lambda = 1.55$ µm. It is clear that the birefringence changes the sign for all indices and it becomes more negative for the greater index and therefore to make it zero again, the width of the rib needs to be increased.

In this section we will study the influence of the waveguide width on the etching depth D, for this all the points of waveguide widths in Figs. 2, 3 and 4, for which the effective index of the fundamental quasi-TE and quasi-TM waveguide modes is equalized, are used to study the influence of the waveguide width on the etching depth D corresponding to $\Delta N = 0$. The variation of the etching depth is shown in Fig. 6. We fit the calculated points by polynomial of degree 2, and we also add simulated zero-birefringence data for waveguide refractive indexes of 1.52, 1.55, and 1.57 and we observed similar trends for all rib refractive indexes.

From Fig. 6, it is clear that as the refractive index n increases, the etch depth (D) decreases, this can be observed for all the zero-birefringence data points and the most important thing is that there is a minimum of each depth D_{min} for each waveguide because the fabrication is easy when the etching depth is small.

And if we consider that the minimum etch depth varies approximately linearly with the refractive index, and after fitting of simulation data, an expression which describes the minimum etch depth for a given waveguide refractive

Fig. 7 Confinement of intensity in the rib waveguide for TE and TM polarizations for four different indexes (1.53, 1.54, 1.56 and 1.57) at $\lambda = 1550$ nm
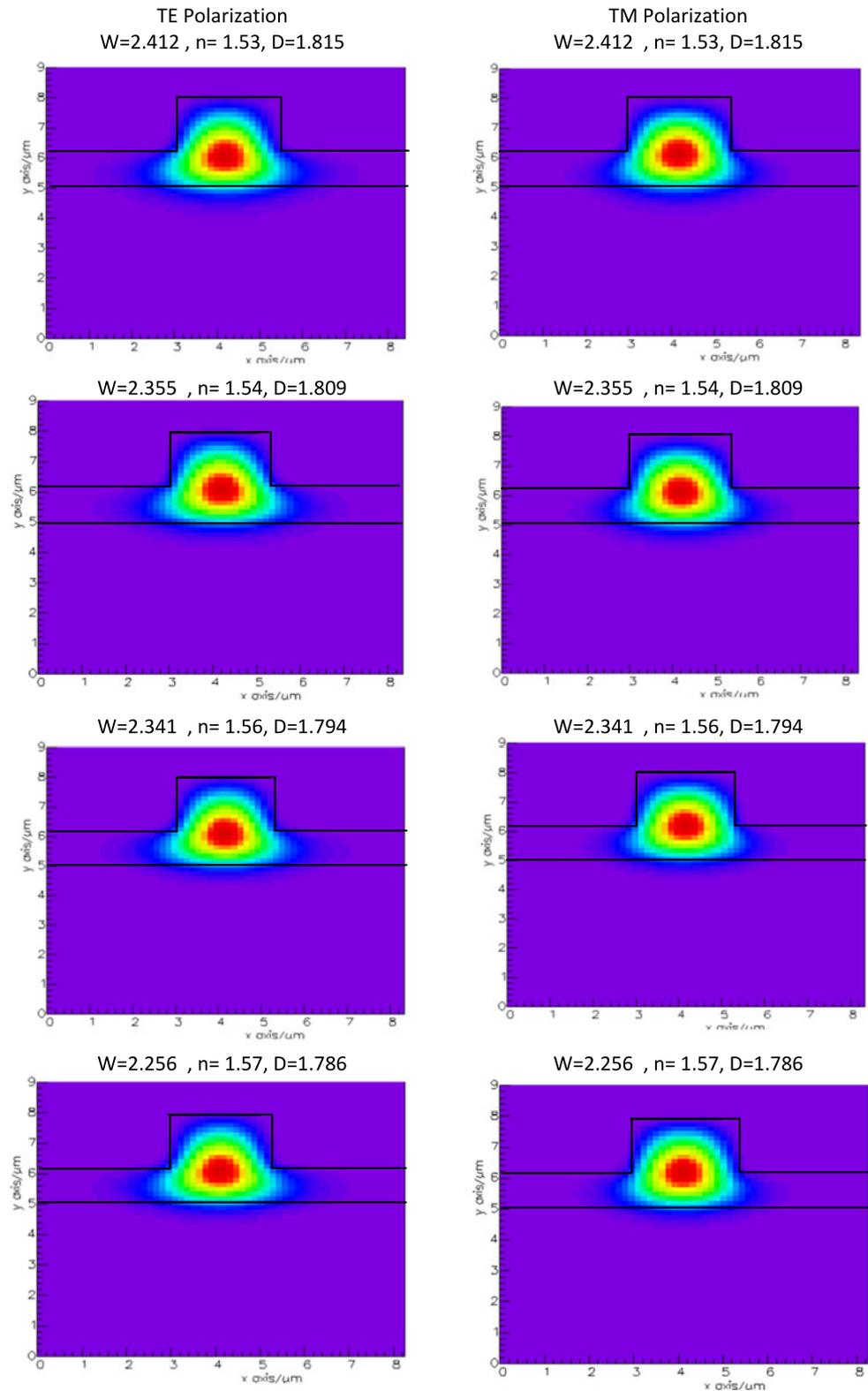
index to predict the zero-birefringence condition is given by

$$D_{\min} \ [\mu m] = 0.24\text{–}0.54n \quad \text{for } \lambda = 1550 \text{ nm} \tag{7}$$

The confinement of intensity in the rib waveguide for TE and TM polarizations for four different indexes (1.53, 1.54, 1.56 and 1.57) at $\lambda = 1550$ nm is shown in Fig. 7. The TE field slightly expands in the thinner active region, and this

effect is more important as the refractive index is reduced. The TM mode appears to be better confined in the central part of the rib waveguide [15].

Increasing the refractive index yields more similar field profiles of the TE and TM modes in the waveguide.

4 Conclusion

An analysis of the modal birefringence between the TE and TM guided modes in SiO_2/ZrO_2 and SiO_2/TiO_2. Thin Film doped with magnetic nanoparticles has been presented using mode solver program to provide theoretical prediction that certain refractive index and waveguide geometries can lead to zero-birefringence condition, the etching depth, width and height values have been determined for different values of refractive index to design waveguides which fulfill this condition, for telecommunication wavelength 1.55 μm.

In the future, such material can find a wide application in optoelectronic devices, and may be interesting to realize waveguides made of magnetophotonic crystals.

References

1. Bahlmann, N., Lohmeyer, M., Zhuromskyy, O., Dotsch, H., Hertel, P.: Nonreciprocal coupled waveguides for integrated optical isolators and circulators for TM-modes. Opt. Commun. **161**, 330–337 (1999)

2. Bahlmann, N., Lohmeyer, M., Zhuromskyy, O., Dotsch, H., Hertel, P.: Integrated magneto-optic Mach-Zehnder interferometer isolator for TE modes. Electron. Lett. **34**, 122 (1998)

3. Lohmeyer, M., Bahlmann, N., Zhuromskyy, O., Doetsch, H., Hertel, P.: Phase-matched rectangular magnetooptic waveguides for applications in integrated optics isolators: numerical assessment. Opt. Commun. **158**, 189 (1998)

4. Chiappini, A., Armellini, C., Chiasera, A., Ferrari, M., Guider, R., Jestin, Y., Minati, L., Moser, E., Nunzi Conti, G., Pelli, S., Retoux, R., Righini, G.C., Speranza, G.: J. Non-Cryst. Solids **355**, 1132–1135 (2009)

5. Royer, F., Jamon, D., Rousseau, J.J., Roux, H., Zins, D., Cabuil, V.: Appl. Phys. Lett. **86**, 011107 (2005)

6. Bentivegna, M.F., Nyvlt, M., Ferre, J., Jamet, J.P., Brun, A., Visnovsky, S., Urban, R.: J. Appl. Phys. **58**, 2270 (1999)

7. Choueikani, F., Royer, F., Jamon, D., Siblini, A., Rousseau, J.J., Neveu, S., Charara, J.: Appl. Phys. Lett. **94**, 051113 (2009)

8. Zayets, V., Debnath, M.C., Ando, K.: Appl. Phys. Lett. **84**, 565 (2004)

9. Amata, H., Royer, F., Choueikani, F., Jamon, D., Broquin, J.E., Plenet, J.C., Rousseau, J.J.: Magnetic nanoparticles doped silica layer reported on ion-exchanged glass waveguide: towards integrated magneto-optical devices. Proc. SPIE **7719** (2010)

10. Chan, S.P., Passaro, V.M.N., Reed, G.T.: Electron. Lett. **41**, 9 (2005)

11. Hocini, A., Boumaza, T., Bouchemat, M., Choueikani, F., Royer, F., Rosseau, J.J.: Appl. Phys. B, Lasers Opt. **99**(3), 553–558 (2010)

12. Sudbø, A.Sv.: IEEE Photonics Technol. Lett. **5**, 342 (1993)

13. FIMMWAVE program. Photon design product. http://www.photond.com

14. Wittekoek, S., Popma, T.J.A., Robertson, J.M., Bongers, P.F.: Magneto-optic spectra and the dielectric tensor elements of bismuth-substituted iron garnets at photon energies between 2.2–5.2 eV. Phys. Rev. B, Condens. Matter **12**, 2777–2788 (1975)

15. Vivien, L., Laval, S., Dumont, B., Lardenois, S., Koster, A., Cassan, E.: Polarization-independent single-mode ribwaveguides on silicon-oninsulator for telecommunication wavelengths. Opt. Commun. **210**, 43–49 (2002)